

Pressure and pressure derivative interpretation of a well in a completed-perforated multilayer reservoir with crossflow

Freddy Humberto Escobar ^a, José Jafet Navia ^a & Daniel Suescún-Díaz ^b

^a Grupo de Investigación GIPE de la Facultad de Ingeniería, Universidad Surcolombiana, Neiva, Colombia. fescobar@usco.edu.co, u20141126880@usco.edu.co

^b Departamento de Ciencias Naturales, Universidad Surcolombiana, Neiva, Huila, Colombia. Daniel.suescun@usco.edu.co

Received: July 22th, 2021. Received in revised form: September 2nd, 2021. Accepted: September 20th, 2021.

Abstract

Various authors have introduced several models for the characterization of multilayer reservoirs. However, some have failed to provide results when the skin factor of the layers is negative. Therefore, in this work, a model applying the concept of the maximum effective hole diameter has been used to simulate pressure tests in multilayer reservoirs. The pressure behavior of such systems is similar to that of naturally fractured double porosity reservoirs. Then, using the unique features of the log-log plot of pressure and pressure derivative versus time, some expressions have been developed to characterize the reservoir. The equations are satisfactorily tested on three field examples. In this way, a more precise reservoir characterization would be achieved, which will imply better reservoir management.

Keywords: interporosity flow parameter; TDS (Tiab's Direct Synthesis) technique; storativity coefficient; semipermeability.

Interpretación de pruebas de presión y derivada de presión en un pozo completamente perforado en un yacimiento multicapa con flujo cruzado

Resumen

Diversos autores han introducido varios modelos para la caracterización de yacimientos multicapas. Algunos modelos no proporcionan resultados cuando el factor de daño de las capas es negativo. En este trabajo, se utiliza un modelo que aplica el concepto de diámetro de pozo máximo efectivo para simular pruebas de presión en depósitos multicapa. El comportamiento de tales sistemas es similar al de los yacimientos naturalmente fracturados de porosidad doble. Luego, utilizando algunas características únicas que se encuentran en la gráfica logarítmica de presión y derivada de presión versus tiempo, se desarrollan algunas expresiones para caracterizar el reservorio. Las ecuaciones se probaron satisfactoriamente en tres ejemplos de campo. De esta manera se lograría una caracterización de yacimiento más precisa que implicará una mejor administración del yacimiento.

Palabras claves: parámetro de flujo interporoso; metodología TDS; coeficiente de almacenaje; semipermeabilidad

1. Introduction

Stratified reservoirs, whose layers or strata have diverse properties, originate due to changes in energy in depositional environments [28]. Studies on these types of systems were first performed in the 1960s. [21] conducted a study on composite stratified reservoirs, i.e., without crossflow. They derived analytical solutions for this type of reservoir,

assuming that the porous volume is filled with a compressible fluid. The authors noted that in an unsteady state, the most permeable layer depletes at a faster rate than the least permeable layer. However, when a steady state is reached, all layers contribute equally to the total reservoir production. Through curves from theoretical pressure buildup tests, they indicated the extent of reservoirs with more than two layers and presented field examples where they applied their

analytical solutions. They found that it was not possible to determine the individual properties of the layers from a pressure buildup curve.

[24] conducted the first study that relates the change in pressure as a function of time to parameters that allow the characterization of reservoirs. An analytical solution that allows extrapolating and estimating the static pressure of the reservoir was proposed; however, this study did not consider fluid compressibility. [23] presented a method for calculating effective permeability from pressure buildup tests. This model considers a uniform formation and a compressible liquid, including biphasic flow. Additionally, [17] developed a method for the estimation of permeability from the slope of the semilog plot. These studies constituted the theoretical basis for the analysis of pressure tests as indicated by [22]. [5] presented a method of interpreting pressure tests, whose basis lies in the rate of change of pressure over time. This study was an important advancement in the interpretation of pressure tests because it was found that the pressure derivative allows a simple and precise distinction of the flow regimes present in the recorded pressure data.

[29] conducted a simplified study of a two-layer horizontal reservoir being depleted by wells completed in both layers. This work did not consider crossflow, that is, the layers only presented communication through the well. Assuming steady-state conditions, they developed simplified analytical solutions with a lower error than the solutions developed for the unsteady state. They reported that the production rate of the well greatly affects the relative depletion of the layers.

[27] and [18] developed the first studies for multilayer crossflow reservoirs. They first developed an analytical solution for a cylindrical reservoir composed of two layers, in which the porous volume is a fluid of constant compressibility. The system is assumed to have a drilled well in the center. They found that for a well producing at constant-pressure conditions, once the unsteady state has been achieved, production declines exponentially. On the other hand, for wells that produce at constant-rate conditions, during the unsteady state, the pressure-time ratio declines linearly. They also reported that during initial production time, a multilayer reservoir with crossflow behaves like a commingled multilayer system, concluding that a multilayer crossflow reservoir can be modeled as a single-layer reservoir, whose properties are the average properties of all layers.

[18] also developed Bessel and Fourier series analytical expressions for the distribution of pressure and flow rate. They demonstrated the applicability of their method by extending the analytical solution of the pressure distribution for cases where more than two layers are present.

[19] developed a numerical model to assess the effect of reservoir stratification on pressure response in flow-restricted wells. They derived equations to determine the appropriate duration of flow and pressure buildup tests in stratified reservoirs. On the other hand, [20] presented methods for determining the individual damage factors and flow capacity of each layer for an infinite reservoir with two layers without crossflow; however, the method can be extended to cases where crossflow occurs. Furthermore, [6] developed a new

model for radial and linear incompressible flow in stratified reservoirs. He evaluated the effect of crossflow on the pressure response and reported the causes of crossflow for a single phase. He also established criteria for the consideration of crossflow during reservoir assessment. The model developed is known as a semipermeable wall model. He found that when a low permeability layer between the layers is not present, the system can be treated as a single-layer system whose permeability corresponds to the average permeability of all layers and the width of the system corresponds to the sum of the layer thicknesses.

[4] developed the double permeability model for multilayer reservoirs with crossflow. He reported that multilayer systems with crossflow do not respond exactly to the heterogeneous reservoir model used to model naturally fractured reservoirs, that is, the double porosity model. He found that the pressure responses of multilayer crossflow reservoirs correspond to intermediate cases between homogeneous reservoirs and double porosity models with interporosity flow conditions. [26] evaluated the pressure response for a two-layer crossflow reservoir, they reported the possibility of estimating the damage factors of each layer from the production data, having used the concept of thick skin to evaluate these types of reservoirs.

[7] studied both cases of stratified systems, i.e., with crossflow and commingled. They presented an analytical solution for a reservoir with n homogeneous layers where crossflow may or may not occur. They included wellbore storage effects for cases where the reservoir is infinite and or has boundaries. [25] conducted a detailed study of the effect of permeability, vertical permeability, skin factors, wellbore storage, layer order, and boundary conditions on pressure response in crossflow multilayer reservoirs. [2] developed an analytical solution for multilayer reservoirs from existing single-layer reservoir solutions, taking into account crossflow between layers. The model was validated using a field example. [1] presented a method for calculating the dimensionless storativity ratio in multilayer deposits with crossflow. Analytic expressions were generated from the separation of the two straight lines presented in the semilog plot of pressure as a function of time. He performed the validation of the information using examples of cases of multilayer reservoirs.

[28] developed the maximum effective hole-diameter model for multilayer crossflow reservoirs in response to the instability in the dual permeability model. That is, the maximum effective hole-diameter model is stable for both positive and negative values of the skin factor. This model was reported by [16] and is the model that will be used in this work for the application of the *TDS* technique [30], with the aim of a better and practical characterizing of multilayer reservoirs with crossflow. [12] also applied the *TDS* technique for the interpretation of pressure tests for a two-layer commingled system separated by a stratum of low permeability. The model was successfully validated using two synthetic examples.

[30] presented a method that allows reservoir characterization without the use of type curves. The method is known as the *TDS* technique and is both practical and accurate. This method uses characteristic points and lines

found on the pressure and pressure derivative log-log plot. Some studies are mentioned regarding this method: [8] applied the *TDS* technique for the interpretation of pressure tests in naturally fractured reservoirs. The method allows a complete characterization of this type of reservoir, as it allows the calculation of parameters necessary for their characterization, such as dimensionless storativity ratio and the interporosity flow parameter, whose correlations were generated by relating the values of these with characteristic values and lines. [11] extended the application of the *TDS* technique to cases of naturally fractured and elongated deposits. The method was validated with field data and synthetic data. [14] applied the *TDS* technique to the analysis of variable flow tests for homogeneous and heterogeneous gas fields. Through simulation runs, the accuracy of the method was demonstrated and verified by synthetic examples. Detailed extension of the *TDS* technique for different cases has also been reported by [9], [10], and [13].

A multilayer reservoir model with all layers being complete, proposed by [16], is employed here to simulate several scenarios and develop the *TDS* technique for this case. The expressions developed were successfully applied to field examples.

2. Mathematical model

[16] presented the Laplacian solution for a well in a two-layer reservoir with crossflow, where both layers are completed:

$$\bar{P}_{wD} = \frac{1}{s} \left(\frac{1}{sC_D + F[(\gamma_1 + \gamma_2 a_1)Y_1 + E(\gamma_1 + \gamma_2 a_2)Y_2]} \right) \quad (1)$$

where,

$$a_j = 1 + \frac{1}{\lambda e^{-2s_{\min}}} \left(\frac{\omega_1 s}{e^{2s_{\min}}} - \gamma_1 \sigma_j^2 \right); \quad j = 1, 2 \quad (2)$$

$$Y_{1,2} = \sigma_{1,2} [K_1(\sigma_{1,2} r_D) - b_{1,2} I_1(\sigma_{1,2} r_D)] \quad (3)$$

$$\sigma_1^2 = 0.5(a + b + \Delta), \quad \sigma_2^2 = 0.5(a + b - \Delta) \quad (4)$$

$$a = \frac{\omega_1 s / e^{2s_{\min}} + \lambda e^{-2s_{\min}}}{\gamma_2} \quad (5)$$

$$b = \frac{\omega_2 s / e^{2s_{\min}} + \lambda e^{-2s_{\min}}}{\gamma_1} \quad (6)$$

$$\Delta = \sqrt{(a - b)^2 + 4(\lambda e^{-2s_{\min}})^2 / \gamma_1 \gamma_2} \quad (7)$$

$$E = \frac{(1 - a_1)X_1 + (S_1' - a_2 S_2')Y_1}{(1 - a_2)X_2 + (S_1' - a_2 S_2')Y_2} \quad (8)$$

$$F = - \frac{(1 - a_2)X_2 + (S_1' - a_2 S_2')Y_2}{a_2(X_1 + S_1'Y_1)(X_2 + S_2'Y_2) - a_1(X_1 + S_1'Y_2)} \quad (9)$$

Variable b in Eq. (3) defines the boundary type. Eq. (10) corresponds to an infinite reservoir, Eq. (11) to a reservoir with a constant pressure limit, and Eq. (12) to a closed reservoir. Note that $k = 1, 2$.

$$b_k = 0 \quad (10)$$

$$b_k = - \frac{K_0(\sigma_k R_{eD})}{I_0(\sigma_k R_{eD})} \quad (11)$$

$$b_k = \frac{K_1(\sigma_k R_{eD})}{I_1(\sigma_k R_{eD})} \quad (12)$$

The dimensionless permeability, dimensionless storativity ratio, and flow capacity ratio are obtained by the following:

$$\lambda = \frac{r_w^2}{(k_1 h_1 + k_2 h_2)} \cdot \tilde{k} \quad (13)$$

$$\omega_j = \frac{(\phi h c_i)_j}{\sum (\phi h c_i)} \quad (14)$$

$$\gamma_j = \frac{(kh)_j}{\sum kh} \quad (15)$$

The dimensionless pressure of layer j , dimensionless pressure derivative, dimensionless radius, dimensionless time, and dimensionless wellbore storage coefficient are defined as follows:

$$P_{Dj} = \frac{\sum kh}{141.2qB\mu} (P_i - P_j) \quad (16)$$

$$t_D * P_{Dj}' = \frac{\sum kh}{141.2qB\mu} (t * \Delta P_j') \quad (17)$$

$$r_D = \frac{r}{r_w e^{-s_{\min}}} \quad (18)$$

$$t_D = \frac{0.0002637t \sum kh}{(\phi h c_i) \mu r_w^2} \quad (19)$$

$$C_D = \frac{0.894C}{\sum (\phi h c_i) r_w^2} \quad (20)$$

3. Formulation

3.1 Dimensionless semipermeability, λ

With a variation in the dimensionless semipermeability in a range from 0.1 to 1×10^{-7} , the pressure derivative curves reported in Fig. 1 were generated. In Fig. 1, it can be observed that the decrease in the value of the dimensionless semipermeability generates a decrease in the value of the minimum (with respect to the axis of the pressure derivative) and its displacement to the right.

As seen in Fig. 2, a direct relationship exists between the dimensionless semipermeability parameter and the minimum dimensionless time, which allows the formulation of the following correlation:

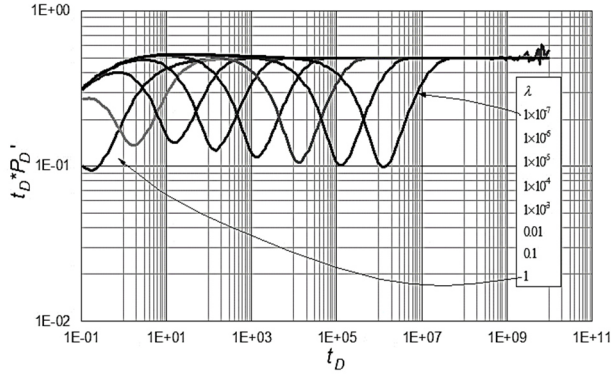


Figure 1. Pressure derivative response for different dimensionless semipermeability values
Source: Authors

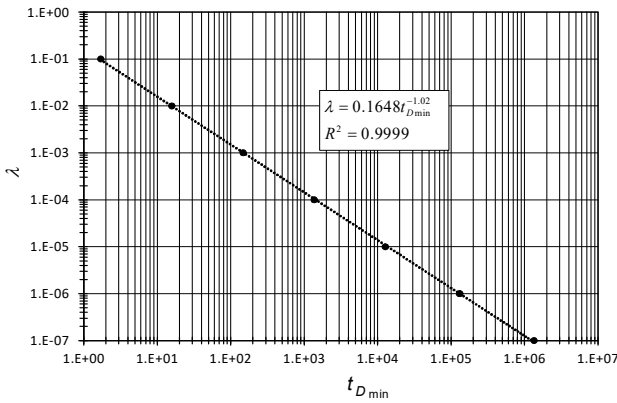


Figure 2. Dimensionless semipermeability as a function of minimum dimensionless time
Source: Authors

$$\lambda = 736.928 \left(\frac{t_{\min} \sum kh}{(\phi h c_t) \mu r_w^2} \right)^{-1.02} \quad (21)$$

In order to provide an interpretation procedure, it is necessary to find a relationship between the semipermeability, pressure derivative, and time. To do so, the affected parameter, which is time, is multiplied by the dimensionless permeability raised to a given power, which is found by either trial and error or using a mathematical procedure as outlined by [15]. The unified pressure derivative behavior is given in Fig. 3, from which the following equation is obtained:

$$(t_D * P_D')_{US} = \frac{1}{2} [\lambda * (t_D)_{US}] \quad (22)$$

Plugging Eqs. (17) and (19) into Eq. (22) and solving for the dimensionless semipermeability yields the following:

$$\lambda = \frac{57.714(\phi h c_t) r_w^2 (t * \Delta P')_{US}}{q B t_{US}} \quad (23)$$

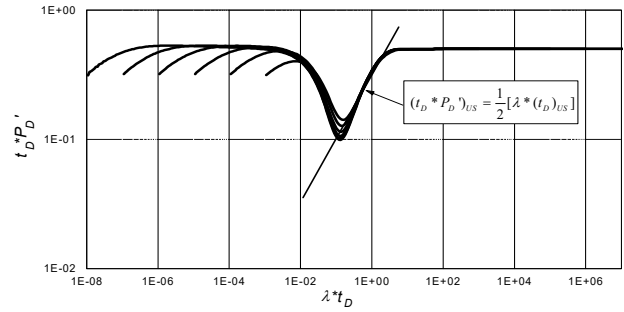


Figure 3. Unified pressure derivative response for different dimensionless semipermeability values
Source: Authors

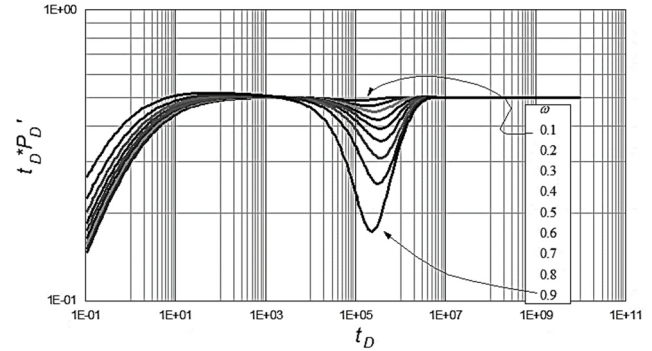


Figure 4. Pressure derivative response for different dimensionless storativity coefficient values
Source: Authors

Intercepting the straight line defined by Eq. (22) with the late radial flow line, which is a horizontal line that intersects in one half, allows the obtaining of another method for estimating the dimensionless semipermeability:

$$\lambda = \frac{1}{(t_D)_{US,i}} \quad (24)$$

After replacing the dimensionless time defined by Eq. (19), the following is derived:

$$\lambda = \frac{3792.2(\phi h c_t) \mu r_w^2}{t_{US,i} \sum kh} \quad (25)$$

3.2 Dimensionless storativity coefficient, ω

To evaluate the effect on the pressure and the pressure derivative responses of the dimensionless storativity coefficient, pressure derivative curves were generated by varying the dimensionless storativity coefficient across a range from 0.1 to 0.9 as reported in Fig. 4.

Fig. 4 shows that increasing the value of the dimensionless storativity coefficient generates a decrease in the value of the minimum of the transition zone with respect to the axis of the pressure derivative.

When plotting the dimensionless storativity coefficient as a function of the ratio of the value of the pressure derivative

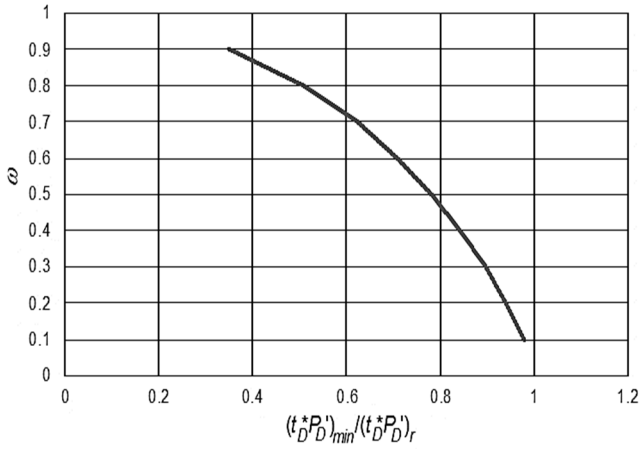


Figure 5. Dimensionless storativity coefficient as a function of the ratio of the minimum pressure derivative value and the pressure derivative during late radial flow regime
Source: Authors

of the minimum of the transition zone with the value of the pressure derivative in the radial flow of the late time (see Fig. 5), we found a correlation that allows the estimation of this parameter with a coefficient of determination of 0.9999999743, that is, Eq. (24).

$$\begin{aligned} \omega = & -1.3770669 \left(\frac{(t^* \Delta P')_{min}}{(t^* \Delta P')_r} \right)^{12} + 3.7786555 \left(\frac{(t^* \Delta P')_{min}}{(t^* \Delta P')_r} \right)^{10} \\ & - 4.0143532 \left(\frac{(t^* \Delta P')_{min}}{(t^* \Delta P')_r} \right)^8 + 1.8333789 \left(\frac{(t^* \Delta P')_{min}}{(t^* \Delta P')_r} \right)^6 \\ & - 0.53251043 \left(\frac{(t^* \Delta P')_{min}}{(t^* \Delta P')_r} \right)^4 - 0.64226552 \left(\frac{(t^* \Delta P')_{min}}{(t^* \Delta P')_r} \right)^2 \\ & + 0.98252485 \end{aligned} \quad (26)$$

Once this value is calculated, it is possible to obtain the individual value of the dimensionless storativity coefficient of the other layer or the other group of layers using Eq. (27).

$$\omega_i = 1 - \omega \quad (27)$$

3.3 Capacity ratio, γ

Similarly, the effect of capacity ratio variation on the pressure derivative response in a multilayer crossflow reservoir was evaluated. The variations were made in a range from 0.01 to 0.9. Fig. 6 indicates that the increase in the value of capacity ratio generates a decrease in the value of the minimum of the transition zone with respect to the axis of the pressure derivative.

After plotting the capacity ratio as a function of the relationship of the value of the minimum pressure derivative of the transition zone and the value of the pressure derivative at the late radial flow regime (see Fig. 7), a correlation was found that allows the calculation of the capacity ratio with a coefficient of determination of 0.999981509, that is, Eq. (28).

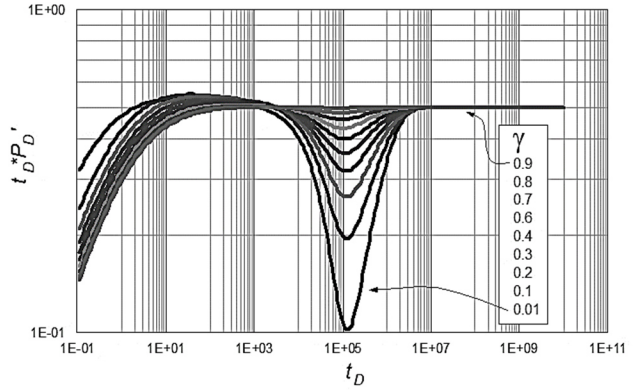


Figure 6. Pressure derivative response of a multilayer crossflow reservoir to changes in the capacity ratio
Source: Authors

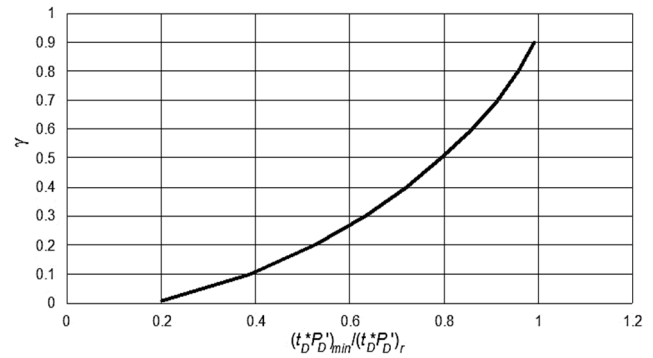


Figure 7. Capacity ratio as a function of the ratio of the minimum pressure derivative value in the transition zone to the value of the pressure derivative during the late radial flow zone
Source: Authors

$$\begin{aligned} \gamma = & 1.8166282 \left(\frac{(t^* \Delta P')_{min}}{(t^* \Delta P')_r} \right)^{10} - 3.9258195 \left(\frac{(t^* \Delta P')_{min}}{(t^* \Delta P')_r} \right)^8 \\ & + 3.2364209 \left(\frac{(t^* \Delta P')_{min}}{(t^* \Delta P')_r} \right)^6 - 1.1283815 \left(\frac{(t^* \Delta P')_{min}}{(t^* \Delta P')_r} \right)^4 \\ & + 0.95708796 \left(\frac{(t^* \Delta P')_{min}}{(t^* \Delta P')_r} \right)^2 - 0.027897437 \end{aligned} \quad (28)$$

The individual capacity ratio of the other layer or the other group of layers can be calculated using Eq. (29):

$$\gamma_i = 1 - \gamma \quad (29)$$

4. Examples

The expressions developed in this study were evaluated using data reported by [1], [4], and [16]. [1] developed correlations for the calculation of the dimensionless storativity coefficient ω in a crossflow reservoir and, in turn, proposed two examples. The schematics of the systems used in Examples 1 and 2 are illustrated in Tables 1 and 2. Example 1 is evaluated by [1] based on the results obtained by [4].

Table 1.
Example 1 parameters

Layer	Parameter	Value
Layer 1	Permeability, κ (md)	200
	Porosity, ϕ	0.25
	Thickness, h (ft)	10
Layer 2	Permeability, κ (md)	1
	Porosity, ϕ	0.15
	Thickness, h (ft)	190

Source: Authors

Table 2.
Example 2 parameters

Layer	Parameter	Value
Layer 1	Permeability, κ (md)	30
	Porosity, ϕ	0.05
	Thickness, h (ft)	10
Layer 2	Permeability, κ (md)	2.5
	Porosity, ϕ	0.18
	Thickness, h (ft)	60
Layer 3	Permeability, κ (md)	30
	Porosity, ϕ	0.05
	Thickness, h (ft)	30
Layer 4	Permeability, κ (md)	2.5
	Porosity, ϕ	0.18
	Thickness, h (ft)	50

Source: Authors

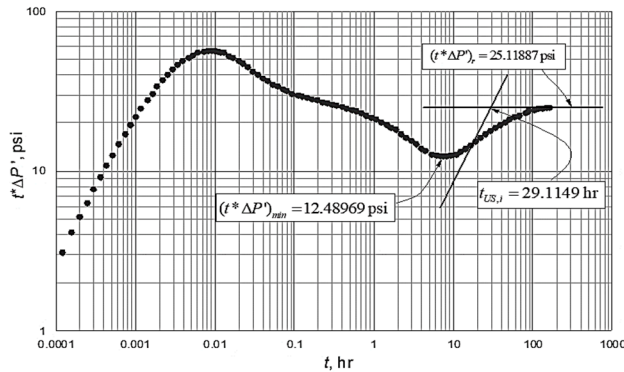


Figure 8. Pressure derivative versus time log-log plot for example 1 reported by [1]

Source: Authors

Table 3.
Results of example 1 using Eqs. 38 and 48 developed by [1] and compared to the theoretical values, the values reported by [4], and the values obtained in this study

	Correla-tion by [1], Eq. (23)	Correla-tion by [1] Eq. (33)	Theoreti-cal values	[4]	This study
λ	-	-	-	-	3.32×10^{-6} , Eq. (21)
λ	-	-	-	-	6.2561×10^{-6} , Eq. (23)
λ	-	-	-	-	6.4233×10^{-6} , Eq. (25)
ω_1	0.078	0.067	0.08064516	0.26	0.192928765
ω_2	0.922	0.933	0.91935484	0.74	0.807071235
γ_1	-	-	0.91324201	-	0.824327546
γ_2	-	-	0.08675799	-	0.175672454

Source: Authors

Table 4.
Results of example 2 of [1] and their comparison with the theoretical values of the parameters and the results obtained in this study.

	Correla-tion by [1], Eq. (28)	Theoreti-cal values	This study
λ	-	-	4.9552×10^{-6} , Eq. (21)
λ	-	-	9.8286×10^{-6} , Eq. (23)
λ	-	-	9.9079×10^{-6} , Eq. (25)
ω_1	0.082	0.09174312	0.302071269
ω_2	0.918	0.90825688	0.697928731
γ_1	-	0.81355932	0.710507243
γ_2	-	0.18644068	0.289492757

Source: Authors

Figs. 8 and 9 show the log-log plots of the pressure derivative versus time for examples 1 and 2, respectively. Table 3 shows the results obtained by [1], the theoretical values, the values reported by [4], and the values obtained using the TDS methodology for Example 1. Table 4 shows the results obtained for Example 2.

The theoretical values were calculated using Eqs. (13), (14), and (15).

When applying the TDS technique, the value calculated using Eq. (26) was found to correspond to ω_2 ; this implies that the storativity coefficient value calculated by Eq. (27) corresponds to ω_1 . A similar case occurred in the calculation of capacity ratio, where the value calculated using Eq. (28) corresponds to γ_2 , and the value calculated using Eq. (29) corresponds to γ_1 .

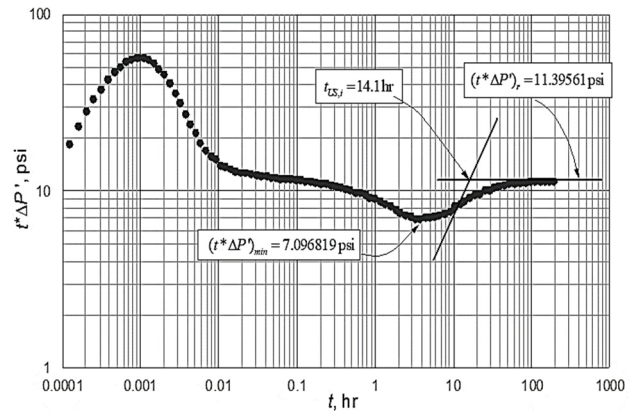


Figure 9. Pressure derivative versus time log-log plot for example 2 reported by [1]

Source: Authors

Table 5.
Results from the double-permeability model by [4] and the results from this study

	[4]	This study
λ	-	1.1913×10^{-9} , Eq. (21)
λ	-	5.9903×10^{-6} , Eq. (23)
λ	1.68×10^{-5}	3.7186×10^{-6} , Eq. (25)
ω_1	0.001	0.098836384
ω_2	0.999	0.901163616
γ_1	0.975	0.925540483
γ_2	0.025	0.074459517

Source: Authors

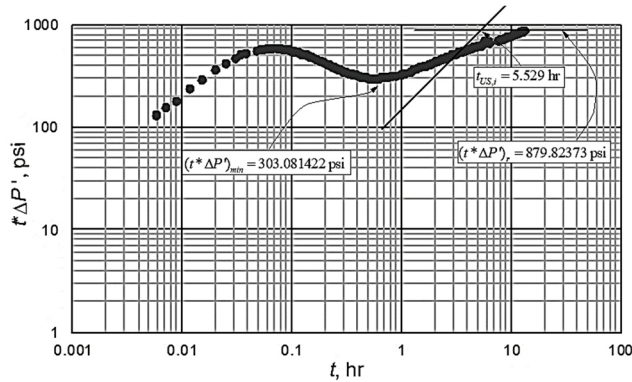


Figure 10. Pressure derivative versus time log-log plot for the case reported by [4]

Source: Authors

As for the example of case 1, the theoretical values were calculated using Eqs. (13), (14), and (15). Like example 1, it was found that the results generated by Eqs. (24) and (26) correspond to the values of ω_2 and γ_2 . In his study, [4] evaluated the double permeability model with a real-field case (see Fig. 10). Table 5 shows the results reported by [4] and those calculated using the expressions developed in this study.

Again, it is pointed out that by calculating the dimensionless storativity coefficient and the capacity ratio, the values calculated using Eqs. (25) and (2) correspond to the values of ω_2 and γ_2 , respectively.

5. Comments on the results

As for the case of the naturally fractured parameters, the results obtained from the worked examples can differ in an order of magnitude. However, the authors consider that the results are very acceptable compared to those obtained from other sources. The unit-slope line during the transition period was not very well defined in all the worked-out exercises. Therefore, the minimum point should be used for these cases for the calculation of the dimensionless semipermeability (Eq. 21).

Synthetic examples were also worked out but not reported here for lack of space. As expected, the simulated results are much closer to the input simulation values. It is also worth mentioning that [3] developed the *TDS* technique for two-layer reservoirs, where the total transmissibility of the formation can be determined from the late radial flow regime. Thus, if the capacity of each layer or group of layers is known, it is possible to determine the transmissibility of each layer.

Based on the foregoing, the application of the correlations generated in this work can provide a more precise characterization of multilayer reservoirs compared to the characterization that can provide double porosity or double permeability models.

6. Conclusions

1. The *TDS* technique was extended to multilayer reservoirs using the model of [16]. Most of the expressions developed correspond to empirical correlations

applicable to field examples. The results obtained are close to results reported from other sources. However, using correlations, it is not possible to determine the layer or group of layers to which the calculated parameter belongs.

2. The correlations developed here can be used together with the *TDS* technique described by [3] for a more complete reservoir characterization because, in late radial flow, the total transmissibility of the formation can be determined. By knowing the capacity of each layer or group of layers, it is possible to know the transmissibility of each layer.

References

- [1] Al-Ajmi, N.M., Kazemi, H. and Ozkan, E., Estimation of storativity ratio in a layered reservoir with crossflow, 2003. in: SPE Annual Technical Conference and Exhibition, October 2003, Denver, Colorado, USA, 2003. DOI: 10.2118/84294-MS.
- [2] Bidaux, P., Whittle, T.M., Coveney, P.J., Gringarten, A.C., Analysis of pressure and rate transient data from wells in multilayered reservoirs: theory and application. in: SPE Annual Technical Conference and Exhibition, October 1992, Washington, D.C., USA, 1992. DOI: 10.2118/24679-MS.
- [3] Bishop, E., Determining individual characteristics of a two layered reservoir using the *TDS* Technique. Dr. Thesis. African University of Science and Technology, Abuja, Nigeria, 2017.
- [4] Bourdet, D., Pressure behavior of layered reservoirs with crossflow, in: SPE California Regional Meeting, March 1985, Bakersfield, California, USA, 1985. DOI: 10.2118/13628-MS.
- [5] Bourdet, D., Ayoub, J.A. and Pirard, Y.M., Use of pressure derivative in well test interpretation. SPE Formation Evaluation, 4, pp. 293-302, 1989. DOI: 10.2118/12777-PA.
- [6] Cheng-Tai, G., Single-phase fluid flow in a stratified porous medium with crossflow (includes associated paper 12946). Society of Petroleum Engineers Journal, 24, pp. 97-106, 1984. DOI: 10.2118/11439-PA.
- [7] Ehlig-Economides, C.A. and Joseph, J., A new test for determination of individual layer properties in a multilayered reservoir. SPE Formation Evaluation 2, pp. 261-283, 1987. DOI: 10.2118/14167-PA.
- [8] Engler, T. and Tiab, D., Analysis of pressure and pressure derivative without type curve matching, 4. Naturally fractured reservoirs. Journal of Petroleum Science and Engineering 15, pp. 127-138, 1996. DOI: 10.1016/0920-4105(95)00064-X.
- [9] Escobar, F., Novel, integrated and revolutionary well test interpretation and analysis, 2019. DOI: 10.5772/intechopen.81078.
- [10] Escobar, F.H., Recent advances in practical applied well test analysis, petroleum science and technology. Nova Science Publishers, Incorporated, 2015.
- [11] Escobar, F.H., Hernández, D.P. and Saavedra, J.A., Pressure and pressure derivative analysis for long naturally fractured reservoirs using the *TDS* technique. DYNA, 77(163), pp. 102-114, 2010.
- [12] Escobar, F.H., Suescún-Díaz, D. and Galindo, J.M., Pressure and pressure derivative analysis with inter-reservoir crossflow rate between adjacent reservoir layers. ARPN Journal of Engineering and Applied Sciences, 15(22), pp. 1120-8415, 2020.
- [13] Escobar, F.H., Jongkittnarukorn, K. and Hernandez, C.M., The power of *TDS* technique for well test interpretation: a short review. Journal of Petroleum Exploration and Production Technology 9, pp. 731-752, 2019. DOI: 10.1007/s13202-018-0517-5
- [14] Escobar, F.H., Sánchez, J.A. and Cantillo, J.H., Rate transient analysis for homogeneous and heterogeneous gas reservoirs using the *TDS* technique. CT&F - Ciencia, Tecnología y Futuro 3, pp. 45-59, 2008.
- [15] Escobar, F.H., Bonilla, L.F. and Hernández, C.M., A practical calculation of the distance to a discontinuity in anisotropic systems from well test interpretation. DYNA, 85(207), pp. 65-73, 2018. DOI: 10.15446/dyna.v85n207.72281.
- [16] Gao, C. and Sun, H., Well test analysis for multilayered reservoirs with formation crossflow, well test analysis for multilayered reservoirs with formation crossflow. 2017. DOI: 10.1016/B978-0-12-812853-4.09976-2

[17] Horner, D.R., Pressure Build-up in wells. Paper presented at the 3rd World Petroleum Congress, The Hague, the Netherlands, 1951.

[18] Katz, M.L. and Tek, M.R., A theoretical study of pressure distribution and fluid flux in bounded stratified porous systems with crossflow. Society of Petroleum Engineers Journal 2, pp. 68-82, 1962. DOI: 10.2118/146-PA.

[19] Kazemi, H. and Seth, M.S., Effect of anisotropy and stratification on pressure transient analysis of wells with restricted flow entry. Journal of Petroleum Technology 21, pp. 639-647, 1969. DOI: 10.2118/2153-PA.

[20] Larsen, L., Determination of skin factors and flow capacities of individual layers in two-layered reservoirs. 1982. DOI: 10.2118/11138-MS.

[21] Lefkovich, H.C., Hazebroek, P., Allen, E.E. and Matthews, C.S., A study of the behavior of bounded reservoirs composed of stratified layers. Society of Petroleum Engineers Journal 1, pp. 43-58. 1961. DOI: 10.2118/1329-G.

[22] Matthews, C.S. and Russell, D.G., Pressure buildup and flow tests in wells, in: Matthews, C.S. and Russell, D.G., Eds., Monograph series. Society of Petroleum Engineers of AIME, 1967.

[23] Miller, C.C., Dyes, A.B. and Hutchinson, C.A., Jr., The estimation of permeability and reservoir pressure from bottom hole pressure build-up characteristics. Journal of Petroleum Technology 2, pp. 91-104, 1950. DOI: 10.2118/950091-G.

[24] Muskat, M., Use of data oil the build-up of bottom-hole pressures. Transactions of the AIME 123, pp. 44-48. 1937. DOI: 10.2118/937044-G.

[25] Park, H. and Horne, R.N., Well test analysis of a multilayered reservoir with formation crossflow, in: SPE Annual Technical Conference and Exhibition, October 1989. San Antonio, Texas, USA, 1989. DOI: 10.2118/19800-MS.

[26] Prijambodo, R., Raghavan, R. and Reynolds, A.C., Well test analysis for wells producing layered reservoirs with crossflow. Society of Petroleum Engineers Journal 25, pp. 380-396, 1985. DOI: 10.2118/10262-PA.

[27] Russell, D.G. and Prats, M., Performance of layered reservoirs with crossflow--single-compressible-fluid case. Society of Petroleum Engineers Journal 2, pp. 53-67, 1962. DOI: 10.2118/99-PA.

[28] Sun, H., Liu, L., Zhou, F. and Gao, C., Exact solution of two-layer reservoir with crossflow under constant pressure condition, in: Society of Petroleum Engineers SPE Latin American and Caribbean Petroleum Engineering Conference - Port-of-Spain, Trinidad and Tobago, 2003. DOI: 10.2118/81043-MS.

[29] Tempelaar-Lietz, W., Effect of Oil production rate on performance of wells producing from more than one horizon. Society of Petroleum Engineers Journal, 1, pp. 26-31, 1961. DOI: 10.2118/1368-G.

[30] Tiab, D., Analysis of pressure and pressure derivatives without type-curve matching: I-skin and wellbore storage, in: SPE Production Operations Symposium, March 1993, Oklahoma City, Oklahoma, USA, 1993. DOI: 10.2118/25426-MS.

Nomenclature

B	Oil volume factor, rb/STB
C	Wellbore storage coefficient, bbl/psi
C_D	Dimensionless wellbore storage coefficient
c_t	Total compressibility, 1/psi
h	Formation thickness, ft
I_0, I_1	Bessel function
k	Permeability, md
\tilde{k}	Semipermeability, md, $\tilde{k} = 2 / (\sigma_1 + \sigma_2)$
K_0, K_1	Bessel function
P	Pressure, psi
P_D	Dimensionless pressure
q	Liquid flow rate, BPD
r	Radius, ft
r_D	Dimensionless radius
r_w	Wellbore radius, ft
R_{eD}	Reservoir dimensionless radius, $R_{eD} = r_e / r_w e^{-s_{min}}$
s	Laplace parameter

S_{min}	Minimum skin factor
S_j	Skin factor of layer j
S'_j	Skin factor of layer j defined by $S'_j = S_j - s_{min}$
t	Time, hr
t_D	Dimensionless time
t_{min}	Time of the minimum pressure derivative, hr
t_{US}	Time during the unit-slope transition period, hr
$t_{DUS,i}$	Intercept of unit-slope during transition period and radial flow, hr
$(t_D * P_D')$	Dimensionless pressure derivative
$(t^* \Delta P')_{min}$	Minimum pressure derivative, psi
$(t^* \Delta P')_r$	Pressure derivative at any point during radial flow regime, psi
$(t^* \Delta P')_{US}$	Pressure derivative during the unit-slope transition period, psi
$(t^* \Delta P')_{US,i}$	Pressure derivative read at the intersect of the unit-slope transition period and radial flow regime, psi

Greek

ω_j	Dimensionless storativity of layer j , defined by Eq. (14)
Δ	Change
ϕ	Porosity, fraction
λ	Dimensionless semipermeability, defined by Eq. (13)
γ_j	Capacity ratio of layer j , defined by Eq. (15)
σ_j	Wall resistance of the layer j , $\sigma_j = h_j/k'$
μ	Viscosity, cp

Suffixes

1, 2	Layers 1 and 2
D	Dimensionless
min	Minimum point
j	Index indicating reservoir layer
r	Radial or pseudorradial
US	Estado pseudoestable
US,i	Intercept of pseudosteady state with radial line
w	Well

F.H. Escobar, is a BSc. Eng in Petroleum Engineer from the Universidad de América in Bogotá, Colombia. He also holds MSc. and PhD. in Petroleum Engineering, both from the University of Oklahoma, USA. He is a professor of the Petroleum Engineering Department in Universidad Surcolombiana, and he is also director of the research group, GIPE (Geoscience, Infrastructure, Productivity and Environment) in the Engineering College of Universidad Surcolombiana, Neiva, Colombia.
ORCID: 0000-0003-4901-6057

J.J. Navia, is a senior student of the Petroleum Engineering Department in Universidad Surcolombiana. He is a member of the Research Group in Universidad Surcolombiana, Neiva, Colombia.
ORCID: 0000-0002-9246-1327

D. Suescún-Díaz is an assistant professor of Nuclear Physics at the Universidad Surcolombiana. He holds two BSc. in Mathematics and Physics from the Universidad Industrial de Santander (UIS), Bucaramanga, Colombia. MSc. in Physics also from UIS. He received his PhD in Physics of Nuclear Reactors at the Federal University of Rio de Janeiro, Brazil and a Postdoc from the same university. His main field of research is computational physics applied to nuclear reactors.
ORCID: 0000-0003-2422-0684